

**© 2018 IEEE.** Personal use of this material is permitted. Permission from IEEE must be obtained for all other uses, in any current or future media, including reprinting/republishing this material for advertising or promotional purposes, creating new collective works, for resale or redistribution to servers or lists, or reuse of any copyrighted component of this work in other works.

Digital Object Identifier (DOI): 10.1109/PESGM.2016.7741327

2016 IEEE Power and Energy Society General Meeting (PESGM)

**LCL filter based UPQC configuration for power quality improvement**

Chandan Kumar

Mahesh K. Mishra

Marco Liserre

**Suggested Citation**

C. Kumar, M. K. Mishra and M. Liserre, "LCL filter based UPQC configuration for power quality improvement," *2016 IEEE Power and Energy Society General Meeting (PESGM)*, Boston, MA, 2016, pp. 1-5.

# LCL Filter Based UPQC Configuration for Power Quality Improvement

Chandan Kumar, *Member, IEEE*, Mahesh K. Mishra, *Senior Member, IEEE*, and Marco Liserre, *Fellow, IEEE*

**Abstract**—This paper proposes a unified power quality conditioner (UPQC) configuration employing an LCL filter at front of shunt voltage source inverter (VSI). As compared to conventional UPQC with L filter at the front of the shunt VSI, the proposed UPQC provides improved compensation while using much smaller value of filter inductance. With the smaller filter inductance, voltage requirement of common dc link also gets reduced. It results in reduced switching losses in the series and shunt VSIs. Therefore, proposed UPQC achieves reduction in weight, cost, size, and losses while providing improved current compensation capability. Simulation results are presented to verify all the features.

**Index Terms:** Power factor, harmonics, voltage regulation

## I. INTRODUCTION

Major power quality (PQ) issues in the power distribution system are unbalanced distorted source current, poor power factor, voltage sag, swell and unbalance, flicker, transients, etc. The unified power quality conditioner (UPQC) has been proposed for simultaneously eliminating these PQ problems with extensive focus on reference generation technique and optimal utilization [1]–[3]. However, the compensation performance of the UPQC largely depends upon the passive filters. These passive filters condition the polluted output of VSI containing higher frequency components, and ensure filtered voltage or current at the PCC.

Presently, almost all UPQC topologies use an L type filter at front of shunt VSI to shape injected currents [1], [2], [4]. The L filter uses a bulky inductor, has a low slew rate for reference tracking, and produces large voltage drop which results in need for higher value of dc link voltage for proper compensation. Another issue with UPQC operation is common dc link voltage requirement. When series and shunt active power filters (APFs) operate separately, both require different voltages at the dc bus [5]. When series and shunt APFs are combined to form UPQC, dc bus voltage is chosen based on requirement of overall performance which uses higher dc voltage rating required by shunt APF. But, higher dc bus voltage increases voltage and power rating of series VSI, increases stress on the VSI switches which in turn increases switching losses, and requires bigger inductor to limit the maximum switching frequency.

Recently, LCL filter has been used at front end of VSI instead of L filter [6]–[8]. This scheme provides better reference

tracking performance while using much lower value of passive components. Also, lower value of passive components ensures that the voltage drop across them is much less. Consequently, the dc link voltage requirement for the LCL filter based shunt VSI will be lesser compared to the L filter based shunt VSI.

Unfortunately, there is lack of literature dealing with the application of LCL filter in the UPQC operation. To fill this gap, this paper proposes a new UPQC configuration integrating an LCL passive filter at the front end of shunt VSI. As compared to conventional UPQC topologies, proposed configuration provides better compensation capability while using smaller value of filter inductance. Therefore, source current quality is improved while reducing the size, weight, and cost of the passive filter. Also, due to requirement of lower dc voltage by LCL filter, losses in both VSIs will decrease. Moreover, performance of the series VSI will also improve while using a smaller inductor.

## II. PROPOSED AND CONVENTIONAL UPQC CONFIGURATION

Equivalent circuit diagram of proposed UPQC configuration is shown in Fig. 1. This consists of two VSIs with a common neutral point clamped dc-link between them. An LCL filter is connected at the front end of shunt VSI. The components  $R_1$  and  $L_1$  are resistance and inductance, respectively at the filter side,  $R_2$  and  $L_2$  are resistance and inductance, respectively at the grid side, and  $C$  is the filter capacitance forming LCL filter part in all three phases. A damping resistance  $R_d$  is used in series with  $C$  to provide passive damping to the overall system. The elements  $L_{se}$ ,  $C_{se}$ , and  $R_{se}$  together form the ripple filter in all three phases which filters out the switching frequency components of the VSI.  $C_{dc}$  is capacitance of both dc link capacitors, whereas a voltage of  $V_{dc}$  is maintained across each of them.

Conventional UPQC topology connects an L filter at the front end of shunt VSI. Filter inductance and resistance of shunt VSI in each phase are given by  $L_f$  and  $R_f$ , respectively.

## III. CONTROL OF THE UPQC

### A. Derivation of Reference Currents of Shunt APF

In this paper, instantaneous symmetrical component theory based control algorithm is used to compute reference filter currents ( $i_{f2j}^*$  where  $j = a, b, c$ ) [9] as follows:

$$i_{f2j}^* = i_{lj} - i_{sj}^* = i_{lj} - \frac{v_{lj1}^+}{\Delta_1^+} (P_{avg} + P_{loss}) \quad (1)$$

where  $\Delta_1^+ = (v_{la1}^+)^2 + (v_{lb1}^+)^2 + (v_{lc1}^+)^2$ . Voltages  $v_{la1}^+$ ,  $v_{lb1}^+$ , and  $v_{lc1}^+$  are fundamental positive sequence voltages at phases

Chandan Kumar is with Electronics and Electrical Engineering Department, Indian Institute of Technology Guwahati, India (e-mail: chandank@iitg.ernet.in).

Mahesh K. Mishra is with Electrical Engineering Department, Indian Institute of Technology Madras, Chennai, India (e-mail: mahesh@ee.iitm.ac.in).

Marco Liserre is Head of Chair of Power Electronics, Christian-Albrechts-Universität zu Kiel, Germany (e-mail: ml@tf.uni-kiel.de).



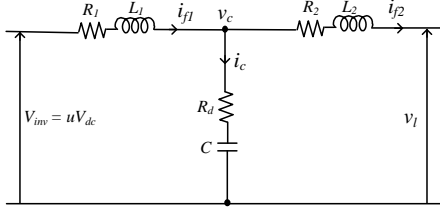


Fig. 3. Single phase circuit diagram of shunt VSI passive filter.

current, resonance frequency ( $f_{res}$ ), choice of damping resistor ( $R_d$ ), and attenuation at switching frequency ( $f_{sw}$ ) [6], [7], [10]. Fig. 3 shows the single phase equivalent circuit of shunt VSI passive filter. Here, inductor  $L_1$  is chosen for attenuation of lower order harmonics. Considering that only  $L_1$  of LCL filter is used, its dynamics is given as

$$L_1 \frac{di_{f1}}{dt} = -v_l - R_1 i_{f1} + V_{inv}. \quad (6)$$

The value of inductance  $L_1$  is chosen from a trade-off, which provides reasonably high switching frequency and sufficient rate of change of filter current, such that the VSI currents follow the reference currents. The inductor is designed to provide good tracking performance at maximum switching frequency which is achieved at the zero of the supply voltage in hysteresis current control (HCC) scheme [11]. Therefore, inductance  $L_1$  is given by

$$L_1 = \frac{V_{dcref}}{(2h_c)(2f_{max})} = \frac{V_{dcref}}{4h_c f_{max}} \quad (7)$$

where  $2h_c$  is allowable ripple in the current and  $f_{max}$  is maximum switching frequency achieved by HCC.

Here, a current ripple of 20% is taken while compromising ripple and inductor size [10]. Substituting values of ripple current and reference dc link voltage  $V_{dcref}$  in (7) while keeping maximum switching frequency ( $f_{max}$ ) at 10 kHz, value of  $L_1$  will be 4.54 mH.

$L_2$  and  $C$  are designed for elimination of higher order harmonics. Without damping resistor while neglecting  $R_1$  and  $R_2$ , expression for the resonance frequency is given as follows:

$$f_{res} = \frac{1}{2\pi} \sqrt{\frac{1+k}{k L_1 C}} \quad (8)$$

where  $k = L_2/L_1$ . Resonance frequency must be greater than the highest order of harmonics current to be compensated. If highest harmonics order to be compensated is 30 and taking a variation of 20%,  $f_{res}$  turns out to be 1800 Hz for a 50 Hz system. For ensuring low loss and high efficiency, a lower value of  $k$  is selected ( $k < 1$ ) [8]. A higher  $C$  will provide a low impedance path for harmonics, but will draw more reactive current from VSI which further increases loss in  $L_1$  and IGBT switch. However, a smaller capacitance will not provide sufficient attenuation which in turn is compensated by selecting larger inductor. As a trade-off between these requirements,  $C = 10 \mu\text{F}$  is chosen. The value of  $k$  is found to be 0.438 using (8). With this value of  $k$ ,  $L_2$  will be 2 mH.

Equivalent impedance of the LCL filter approaches to zero at the resonance frequency ( $f_{res}$ ) and system may become

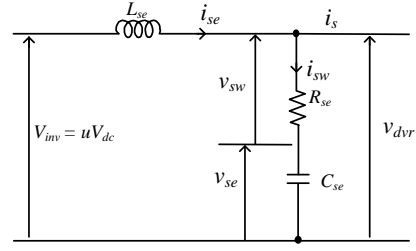


Fig. 4. Single phase equivalent circuit of series VSI passive filter.

unstable. However, system can be made stable by inserting a resistance ( $R_d$ ) in series with the capacitor. Usually, it is chosen more than the capacitive reactance at  $f_{res}$  ( $X_{cres}$ ) such that the damping losses are minimum while assuring that the sufficient resonance damping is provided to the system [12].

### C. Design of Parameters of Series APF

Single phase circuit diagram of passive filter of series APF is given in Fig. 4. A detailed design procedure has been presented in following section [13].

1) *Design of Inductor ( $L_{se}$ ):* At any point of time, inductor dynamics is represented by following equation:

$$L_{se} \frac{di_{se}}{dt} = -v_{dvr} + V_{dcref} \quad (9)$$

where  $i_{se} = i_s + i_{sw}$ . Practically, source current variations are much slower as compared to the capacitor current. Therefore,  $\frac{di_{se}}{dt} = \frac{d(i_{sw} + i_s)}{dt} \approx \frac{di_{sw}}{dt}$ . Replacing this expression in (9)

$$L_{se} \frac{di_{sw}}{t_{on}} = V_{dcref} - v_{dvr}. \quad (10)$$

Assuming that the rate of change of capacitor current is same in both ON as well as OFF switching state, switching frequency  $f_{sw}$  can be given as follows:

$$f_{sw} = \frac{V_{dcref} - v_{dvr}}{2 L_{se} di_{se}}. \quad (11)$$

From Fig. 4, voltage across the DVR is given as

$$v_{dvr} = R_{se} i_{sw} + \frac{1}{C_{se}} \int i_{sw} dt \quad (12)$$

Differentiating above equation with respect to time

$$\frac{dv_{dvr}}{dt} = R_{se} \frac{di_{sw}}{dt} + \frac{1}{C_{se}} i_{sw}. \quad (13)$$

The capacitor will draw negligible current at lower order harmonics, and will provide a low impedance path at higher order harmonics. Thus, voltage drop across the capacitor will be negligible at the higher order harmonics. Moreover, drop across resistor will be predominant at higher order frequencies and will be nearly equal to  $2h_v$ . Hence, (13) becomes

$$di_{sw} = \frac{2h_v}{R_{se}}. \quad (14)$$

Substituting (14) into (11)

$$f_{sw} = \frac{R_{se}}{4 L_{se} h_v} [V_{dcref} - v_{dvr}]. \quad (15)$$

TABLE I  
SIMULATION PARAMETERS

System quantities	Values
Source voltage	230 V rms line to neutral, 50 Hz
Feeder parameters	$R_s = 0.5 \Omega$ , $L_s = 0.5$ mH
Linear load	$Z_{la} = 20 + j94.2 \Omega$ , $Z_{lb} = 40 + j62.8 \Omega$ , $Z_{lc} = 50 + j94.2 \Omega$
Nonlinear load	$R_{nl} = 50 \Omega$ , $L_{nl} = 300$ mH
UPQC parameters (conventional scheme)	$V_{dcref} = 520$ V, $C_{dc} = 2500$ $\mu$ F, $L_f = 23.6$ mH, $R_f = 0.5 \Omega$ $L_{se} = 6.93$ mH, $C_{se} = 30$ $\mu$ F, $R_{se} = 3.68 \Omega$
UPQC parameters (proposed topology)	$V_{dcref} = 400$ V, $C_{dc} = 2500$ $\mu$ F, $L_1 = 4.5$ mH, $L_2 = 2$ mH, $R_d = 25 \Omega$ , $R_1 = R_2 = 0.5 \Omega$ , $C = 10$ $\mu$ F, $L_{se} = 5.5$ mH, $C_{se} = 30$ $\mu$ F, $R_{se} = 3.68 \Omega$

In above equation, maximum switching frequency can be achieved for  $v_{dvr} = 0$ . Hence, filter inductance to limit maximum VSI frequency is given as following:

$$L_{se} = \frac{V_{dcref} R_{se}}{4 h_v f_{max}}. \quad (16)$$

2) *Design of Capacitor and Resistor ( $C_{se}$  and  $R_{se}$ ):* As already mentioned, the values of capacitor and resistor are chosen such that the voltage drop across the resistor will be much more than that the voltage across capacitor at the higher order frequency component. Therefore, series filter circuit acts as a first order circuit and makes voltage-current relation linear.

With UPQC in operation, source will supply only fundamental positive component of load currents. Consider  $I_s$  and  $I_{se}$  as rated currents to be drawn from source and current rating of the series VSI, respectively. Therefore, maximum current that can flow through the series capacitor  $C_{se}$  will be  $I_{sw} = \sqrt{I_{se}^2 - I_s^2}$ . At fundamental frequency, the voltage drop across resistor is negligible as compared to the capacitor, whereas at higher frequencies the voltage drop across capacitor is negligible compared to resistor. Therefore,  $I_{sw}$  can be divided into parts 1) fundamental current corresponding to voltage across capacitor ( $I_{sw1}$ ); and 2) switching frequency current ( $I_{swh}$ ). Therefore,  $I_{sw} = \sqrt{I_{sw1}^2 + I_{swh}^2}$ .

Neglecting voltage drop across resistor at fundamental frequency, voltage across capacitor is given as

$$V_{se} = V_{dvr} = I_{sw1} X_{se1} = \frac{I_{sw1}}{2\pi f_1 C_{se}}. \quad (17)$$

Restricting total reactive current drawn by the capacitor to 5% of the rated load current, capacitor value will be

$$C_{se} = \frac{I_{se}}{40\pi f_1 V_{ref1}}. \quad (18)$$

Further, neglecting capacitor voltage drop at higher frequency component, voltage across resistor is given as:

$$V_{sw} = I_{seh} R_{sw}. \quad (19)$$

At the switching frequency, the rms value of  $V_{sw}$  will be  $h_v/\sqrt{3}$ . Restricting total current drawn by the resistor to 5% of the rated current, the value of resistor is given as

$$R_{sw} = \frac{20 h_v}{\sqrt{3} I_{se}}. \quad (20)$$

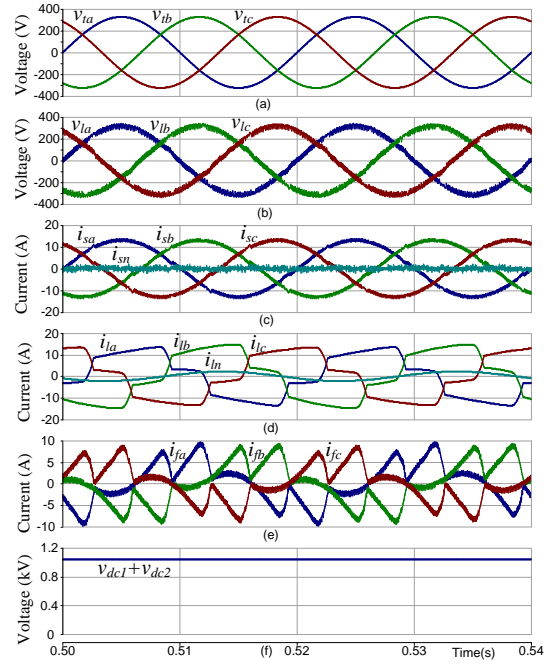


Fig. 5. Compensation performance of conventional UPQC. (a) PCC voltages. (b) Load voltages. (c) Source currents. (d) Load currents. (e) Shunt VSI currents. (f) Voltage at dc link. ( $L_f = 23.6$  mH and  $L_{se} = 6.93$  mH).

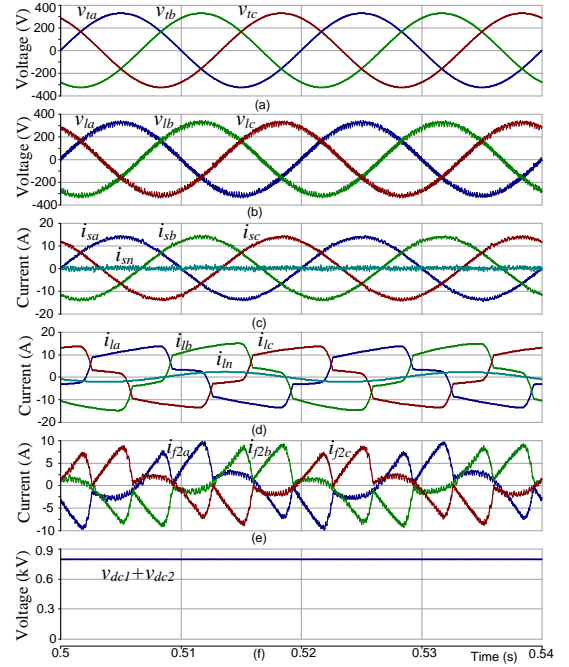


Fig. 6. Compensation performance of proposed UPQC. (a) PCC voltages. (b) Load voltages. (c) Source currents. (d) Load currents. (e) Shunt VSI currents. (f) Voltage at dc link. ( $L_1 = 4.5$  mH,  $L_2 = 2$  mH,  $C = 10$   $\mu$ F,  $L_{se} = 5.5$  mH).

## V. SIMULATION RESULTS

Firstly, steady state compensation performance of conventional scheme is shown in Fig. 5. As can be seen from the figure that the load voltages and source currents are balanced, sinusoidal, and in phase with the respective phases. However, these waveforms contain switching harmonic ripple

TABLE II  
PERCENTAGE THDS IN SOURCE CURRENTS AND LOAD VOLTAGES

System configuration	$i_{sa}$	$i_{sb}$	$i_{sc}$	$v_{la}$	$v_{lb}$	$v_{lc}$
Without compensation	20.69	18.41	20.1	1.05	1.04	1.03
Compensation with conventional topology	2.3	2.2	2.05	1.13	1.11	1.05
Compensation with proposed topology	1.12	1.1	1.08	0.8	0.75	0.72

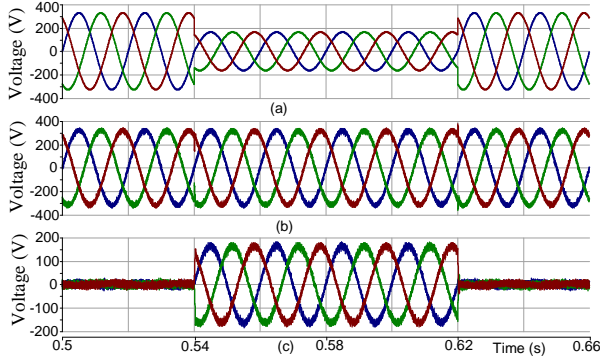


Fig. 7. Compensation performance of proposed UPQC during voltage sag. (a) PCC voltages. (b) Load voltages. (c) DVR injected voltages.

TABLE III  
COMPARISON OF UPQC PARAMETERS

UPQC topology	Shunt VSI inductor	Series VSI inductor	Voltage at dc link
Conventional	23.6 mH	6.93 mH	1040 V
Proposed	6.5 mH	5.5 mH	800 V

component. Moreover, total dc link voltage is maintained at the reference value of 1040 V to achieve this compensation.

Fig. 6 illustrates the steady state simulation waveforms for the proposed UPQC configuration. The waveforms of three phase source voltages, load voltages, source currents, load currents, shunt VSI currents, and voltage at dc link are shown in Figs. 6(a)-(f), respectively. The load voltages and source currents are balanced, sinusoidal, and in phase with respective phases. Moreover, these waveforms have reduced switching ripple components as compared to the waveforms of conventional scheme as shown in Fig. 5. Consequently, the filter currents injected at the load point have reduced harmonic ripple component in the proposed scheme. A total voltage of 800 V (400 V across each capacitor) is maintained at the common dc link of the VSIs, and it is sufficient to achieve improved compensation performance. For the comparison purpose, the percentage total harmonic distortion (THDs) level of source currents and load voltages in conventional and proposed UPQC schemes are given in Table II. It can be observed that the percentage THDs of source currents have been decreased in the proposed scheme. Further, Table III summarizes the details of filter inductances of passive filter components and total dc link voltage in both the schemes.

Proposed UPQC configuration is subjected to three phase voltage sag of 50% as shown in Fig. 7. Compensated load voltages maintained at the reference voltage are given in 7(b), whereas voltages injected by the series transformer are shown in 7(c). These results show the capability of proposed scheme to effectively compensate for voltage disturbances.

## VI. CONCLUSIONS

This paper proposes a UPQC configuration employing an LCL input filter at the front end of shunt VSI to mitigate voltage and current related PQ problems. Proposed UPQC has provided better current and voltage compensation with improved ripple attenuation capability while using reduced passive components. Moreover, appropriate reduction in common dc link voltage is also achieved. With the simulation results, it is verified that the proposed UPQC configuration is able to provide improved compensation while utilizing reduced size passive components and dc link voltage as compared with the conventional UPQC.

## REFERENCES

- [1] V. Khadkikar and A. Chandra, "UPQC-S: A novel concept of simultaneous voltage sag/swell and load reactive power compensations utilizing series inverter of UPQC," *IEEE Trans. Power Electron.*, vol. 26, no. 9, pp. 2414–2425, Sep. 2011.
- [2] M. Kesler and E. Ozdemir, "Synchronous-reference-frame-based control method for UPQC under unbalanced and distorted load conditions," *IEEE Trans. Ind. Electron.*, vol. 58, no. 9, pp. 3967–3975, Sep. 2011.
- [3] G. Kumar, B. Kumar, and Mahesh K. Mishra, "Mitigation of voltage sags with phase jumps by UPQC with PSO-based ANFIS," *IEEE Trans. Power Del.*, vol. 26, no. 4, pp. 2761–2773, Oct. 2011.
- [4] V. Kinhal, P. Agarwal, and H. Gupta, "Performance investigation of neural-network-based unified power-quality conditioner," *IEEE Trans. Power Del.*, vol. 26, no. 1, pp. 431–437, Jan. 2011.
- [5] A. Bhattacharya, C. Chakraborty, and S. Bhattacharya, "Parallel-connected shunt hybrid active power filters operating at different switching frequencies for improved performance," *IEEE Trans. Ind. Electron.*, vol. 59, no. 11, pp. 4007–4019, Nov. 2012.
- [6] M. Tavakoli Bina and E. Pashajavid, "An efficient procedure to design passive LCL-filters for active power filters," *Electric Power Systems Research*, vol. 79, no. 4, pp. 606–614, 2009.
- [7] O. Vodyakho and C. Mi, "Three-level inverter-based shunt active power filter in three-phase three-wire and four-wire systems," *IEEE Trans. Power Electron.*, vol. 24, no. 5, pp. 1350–1363, May 2009.
- [8] Chandan Kumar and Mahesh K. Mishra, "An improved hybrid DSTATCOM topology to compensate reactive and nonlinear loads," *IEEE Trans. Ind. Electron.*, vol. 61, no. 12, pp. 6517–6527, Dec. 2014.
- [9] A. Ghosh and G. Ledwich, *Power Quality Enhancement Using Custom Power Devices*. Kluwer Publications, 2002.
- [10] M. Liserre, F. Blaabjerg, and S. Hansen, "Design and control of an LCL-filter-based three-phase active rectifier," *IEEE Trans. Ind. Appl.*, vol. 41, no. 5, pp. 1281–1291, Sep. 2005.
- [11] Mahesh K. Mishra and K. Karthikeyan, "An investigation on design and switching dynamics of a voltage source inverter to compensate unbalanced and nonlinear loads," *IEEE Trans. Ind. Electron.*, vol. 56, no. 8, pp. 2802–2810, Aug. 2009.
- [12] R. Beres, X. Wang, F. Blaabjerg, M. Liserre, and C. Bak, "Optimal design of high-order passive-damped filters for grid-connected applications," *IEEE Trans. Power Electron.*, vol. 31, no. 3, pp. 2083–2098, Mar. 2016.
- [13] S. Sasitharan and Mahesh K. Mishra, "Constant switching frequency band controller for dynamic voltage restorer," *Power Electronics, IET*, vol. 3, no. 5, pp. 657–667, Sep. 2010.